

Quantitative Single Molecule Surface-Enhanced Raman Scattering by Optothermal Tuning of DNA Origami Assembled Plasmonic Nanoantennas

Sabrina Simoncelli^{1‡}, Eva-Maria Roller^{2‡}, Patrick Urban¹, Robert Schreiber⁴, Andrew J. Turberfield⁴, Tim Liedl^{2,3} and Theobald Lohmüller^{1,3*}*

¹Photonics and Optoelectronics Group, Department of Physics and Center for Nanoscience (CeNS), Ludwig-Maximilians-Universität München, Amalienstraße 54, Munich, 80799, Germany

²Department of Physics and Center for Nanoscience (CeNS), Ludwig-Maximilians-Universität München, Geschwister-Scholl-Platz 1, Munich, 80539, Germany

³Nanosystems Initiative Munich (NIM), Schellingstraße 4, 80539 Munich, Germany

⁴Clarendon Laboratory, Department of Physics, University of Oxford, Parks Road, Oxford OX1 3PU, United Kingdom

[‡]These authors contributed equally to this work

Abstract: DNA origami is a powerful approach for assembling plasmonic nanoparticle dimers and Raman dyes with high yields and excellent positioning control. Here we show how optothermal induced shrinking of a DNA origami template can be employed to control the gap sizes between two 40 nm gold nanoparticles in a range of 1 nm – 2 nm. The high field confinement achieved with this optothermal approach was demonstrated by detection of surface-enhanced Raman spectroscopy (SERS) signals from single molecules that are precisely placed within the DNA origami template that spans the nanoparticle gap. By comparing the SERS intensity with respect to the field enhancement in the plasmonic hot-spot region, we found good agreement between measurement and theory. Our straightforward approach for the fabrication of addressable plasmonic nanosensors by DNA origami demonstrates a path toward future sensing applications with single-molecule resolution.

Keywords: SERS, DNA Origami, single molecule, plasmonic heating

DNA origami¹⁻² allows to design three dimensional structures of various materials and functionalities with nanoscale accuracy.³⁻⁷ This broad versatility has been employed in numerous scientific applications in such diverse fields as (bio)sensing,⁸⁻¹⁰ catalysis,¹¹ nanomedicine,¹²⁻¹⁵ and super-resolution microscopy.¹⁶⁻¹⁷ In recent years, DNA origami has also been used to assemble complex and multifunctional plasmonic nanostructures such as plasmonic nanoparticle rings,¹⁸ helices¹⁹ as well as reconfigurable plasmonic metamolecules,²⁰ and for studying enhanced light matter interactions between plasmonic nanoantennas and single molecules.²¹

Plasmonic nanoparticles or nanoantennas are capable of concentrating far field propagating light into a nanoscale volume.²² If two gold nanoparticles (AuNPs) are brought into close proximity, the plasmonic coupling between them results in a strong enhancement of the electric field in the nanoparticle gap.²³ The magnitude and spatial distribution of this so-called plasmonic ‘hot-spot’ is a consequence of the particle size and separation distance.²⁴ However, any target molecule must be positioned precisely between the two particles to benefit from the strongest signal enhancement. Controlling these parameters is challenging, but DNA origami has shown to be well suited for addressing this problem. Dimer antennas made of two plasmonically coupled gold nanoparticles that were assembled by DNA origami have been used to significantly enhance fluorescence intensity²¹ and the surface-enhanced Raman scattering (SERS) signal from molecules that were located in the nanoparticle gap.²⁵⁻²⁸ Particularly SERS-substrates often face the problem of poor reproducibility and performance since the Raman scattering cross-sections of most molecules are orders of magnitude smaller than the cross-section for fluorescence.²⁹ Detecting Raman signals therefore relies on very high field enhancements, which is associated with an extremely small gap size of only a few nanometers. It has been shown that DNA scaffolds can be employed to align two gold nanoparticles in close proximity by either positioning them on the surface of a

DNA sheet,²⁸ or by connecting them on both sides of a DNA stack that spans the nanoparticle gap.²⁶ For molecules that are embedded in the origami structure, the latter design comes with the benefit that the analyte is located precisely at the area of the largest field enhancement (Figure 1). DNA origami designs with a nanoparticle gap between 3 nm – 5 nm have been reported to provide large SERS enhancements of up to seven orders of magnitude, which was, however, not sufficient to achieve single molecule sensitivity.³⁰ Nanoparticle dimer structures with gap sizes < 2 nm have shown to be suitable for single-molecule SERS.³¹⁻³⁴ Yet in all cases, the additional growth of a silver layer on top of the AuNP dimers was necessary to reduce the particle spacing, which is a huge disadvantage, particularly for biological applications. In order to avoid any chemical treatment and to boost the field enhancement in the hot-spot for quantitative single-molecule detection, it is thus pivotal to reduce the separation distance between two gold nanoparticles in a range between 1 nm and 2 nm.

An alternative strategy to growing a shell around the particles is to bring them closer together by reducing the thickness of the origami template. Heating of temperature sensitive polymer sheets, for example, has shown to be an effective way to reduce the separation distance between optically printed nanoparticle dimers and tetramers.³⁵ Pillers *et al.*³⁶ and Kim *et al.*,³⁷ have reported that heating of DNA origami sheets above 150°C results in uniform shrinking of the height of the structures by roughly 50 %. In a similar way, this temperature induced shrinking could thus be applied as an experimental strategy to reduce the effective separation distance between two nanoparticles that are aligned by a DNA scaffold.

Heating is in fact a limiting parameter for any SERS measurement that employs plasmonic nanoparticle structures. For Raman measurements, the irradiation with laser light is imperative. Light absorbed by gold nanoparticles, however, is converted into heat.³⁸⁻³⁹ Furthermore, the highest SERS enhancement is expected if the laser wavelength is resonant

with the nanoparticle plasmons, which is also the regime for most efficient plasmonic heating. Temperatures up to several hundred degrees Kelvin can be reached if the laser power is too high, which can immediately result in the destruction of the sample. Controlled laser illumination, however, can also be employed to deposit a defined amount of heat in a nanoscale region around the particles.

Here, we demonstrate that optothermal induced shrinking of a DNA origami template in between two gold nanoparticles can be employed to reduce the gap-size to sub-two-nanometer dimensions and hence increase the field enhancement in the nanoparticle gap. The gap size reduction was investigated by far field scattering measurements of individual dimer nanoantennas in combination with Raman measurements. With this approach, we were able to quantitatively map the increase of the SERS signal intensity from a single molecule that is placed in the hot spot between both particles as a function of the nanoparticle spacing and found good agreement between experiment and theory.

Results

DNA origami AuNP dimers design and fabrication.

The design of a gold dimer structure assembled on a DNA origami template is shown in Figure 1. Two gold nanoparticles of 40 nm diameter were aligned in close proximity by the help of a stack of five DNA layers with outer dimensions of 47 nm x 44 nm. Out of these five DNA layers only the middle one forms a complete sheet (see Supporting Figure 1). The other layers have a frame like shape so that the complete DNA origami structure offers two funnel-forming grooves (see Figure 1b). The DNA origami has a two-fold function. On the one hand, each of the grooves is designed to perfectly embed the 40 nm AuNPs, which leads to a rigid AuNP dimer configuration. On the other hand, there is one layer of DNA in the middle of the hot spot that offers the possibility to have site-specific binding of any molecule of

interest. This strategy allows placing a controllable number of Raman reporter molecules precisely in the region of the highest electromagnetic field (for a detailed protocol of the DNA origami dimer self-assembly see the Methods section). Here, we directly modified either one or four DNA staple strands incorporated into this middle DNA layer with a Cy3 or Cy3.5 molecule (see Figure 1b). The different dimer structures with their specific type and number of dye molecules in the hot spot region were prepared in separate batch reactions. The final structures were subsequently drop-cast on a clean glass coverslide, incubated for 5 min and dried with nitrogen. Figure 1a and Supporting Figure 2 and 3 show representative transmission electron microscopy (TEM) images of the DNA origami AuNP dimer structures. The average gap size of dried DNA origami AuNP dimers was $\sim 2.8 \pm 1$ nm.

Plasmonic heating and surface-enhanced Raman scattering.

A schematic overview of the experimental approach is shown in Figure 2a. The measurement for a single dimer was conducted in a sequence of measurement and heating steps; both Raman scattering and heating were performed with a continuous-wave 612 nm laser. The scattering spectra of an individual DNA origami dimer modified with only one Cy3.5 molecule placed in the center of the hot spot is shown in Figure 2b. Before laser irradiation, the scattering spectrum of the dimer displayed a resonance at 592 nm (Figure 2b, black line). The corresponding Raman spectra of Cy3.5 did not show any visible peaks (Figure 2c, black line). Raman measurements were carried out at a low excitation intensity of $\sim 14 \text{ kW/cm}^2$ to avoid heating of the sample. Control measurements of the scattering spectra before and after the Raman measurement were taken to ensure that the laser illumination during the Raman measurement did not cause any change or deterioration of the sample. In the next step, the same dimer structure was irradiated with a four times higher laser power density (60 kW/cm^2) for 10 seconds. After the first of such a heating step, the scattering peak displayed a red shift from 592 nm to 618 nm (Figure 2b, green line), indicative of a reduction

of the nanoparticle gap and increased plasmonic coupling. When repeating the Raman measurement, peaks for the single Cy3.5 dye (952, 1195, 1357 cm^{-1}) were now observed in the spectrum (Figure 2c, green line). The intensities of these Raman peaks improved further after repeating the heating step for a second time. Also the scattering peak of the gold dimer structure was red-shifted again by about 30 nm from 618 nm to 637 nm (Figure 2b, red line) indicating even stronger plasmonic coupling. In addition, the emergence of a smaller peak at ~ 555 nm was observed, corresponding to the transverse plasmon mode along the short axis of the dimer structure. The new Raman spectrum again displayed a strong increase of the peak intensities as a result of the much stronger field enhancement in the nanoparticle gap (Figure 2c, red line).

The detected Raman signals were stable and only limited by bleaching of the dye. The recorded Raman scattering signals showed the characteristic spectral fluctuations associated with single-molecule SERS.⁴⁰ Cy3.5 is a Raman analyte with many characteristic fingerprints. We identified typical Cy3.5 vibrational modes located at \sim (960, 1180, 1280, 1315, 1350, 1390, 1430, 1470, 1520, 1550, 1590, 1600, 1620) cm^{-1} for gap sizes smaller than 2.5 nm. For instance, the peak located at ~ 960 cm^{-1} is expected to arise from the vibrational modes of the central π -conjugated chain,⁴¹ whereas the peak at ~ 1280 cm^{-1} corresponds to the motions of the ethyl groups attached to the aromatic moiety.⁴² The peak located at ~ 1350 cm^{-1} can be assigned to the methine chain motions of the cyanine dye⁴²⁻⁴³ and the peaks at ~ 1390 and 1470 cm^{-1} correspond to the CH_3 symmetric and asymmetric deformation modes, respectively.⁴²⁻⁴³ Features between 1550 and 1590 cm^{-1} are associated to the $\text{N}^+=\text{C}$ stretching motion,⁴²⁻⁴⁴ those at ~ 1600 and 1620 cm^{-1} can be attributed to the $\text{C}=\text{C}$ stretching mode.⁴⁴ We also observed some peaks related to the vibrational modes of DNA \sim (760, 1030, and 1580 cm^{-1}).⁴⁵⁻⁴⁶ The peaks located at 760 and 1030 cm^{-1} are thought to arise from the ring breathing⁴⁷ and a methyl rocking vibration of the thymine nucleotide,⁴⁸ respectively.

The peak at 1580 cm^{-1} corresponds to the ring stretching of adenine nucleotides as well as the N6H₂ deformation.⁴⁷ Further, the peak located at $\sim 1090\text{ cm}^{-1}$ corresponds to the vibrational mode originated from the symmetric stretching vibration of the phosphodioxo- (PO_2^-) DNA backbone.^{45-46, 49}

We inferred the gap sizes for individual DNA AuNP dimers from their Rayleigh scattering spectra using Mie theory.⁵⁰⁻⁵¹ According to the data shown in Figure 2b and our numerical simulations, the gap size was reduced from $\sim 3.3\text{ nm}$ to 1.9 nm and from $\sim 1.9\text{ nm}$ to 1.3 nm in the first and second round of laser heating, respectively. We did not observe any melting or re-shaping of the gold particles after laser treatment as verified by SEM and TEM measurements. The observed red shift of the plasmon resonance can therefore be attributed solely to the irreversible reduction of the nanoparticle gap by optothermal induced shrinking of the DNA template. The structural stability of the DNA origami template depends on temperature. For temperatures beyond 200°C thermally induced structural changes are reflected in a change of the AuNP dimer gap size. However, the extent of the plasmonic shift and gap size reduction varies between 20 % and 40 % from dimer to dimer as confirmed by Rayleigh scattering spectroscopy and TEM imaging (see Supporting Figure 4). Yet, a gradual red-shift of the scattering peak due to a reduction of the nanoparticle gap, as schematically depicted in Figure 2a was observed for all samples.

We performed numerical simulations to estimate the increase in temperature of the nanoparticle dimer (see Methods section and Supporting Figure 5). The maximum temperature of the structure for the radiant flux density of $\sim 14\text{ kW/cm}^2$ (used for Raman measurements) is lower than 200°C independently of the initial position of the longitudinal plasmonic mode. For an excitation intensity of $\sim 60\text{ kW/cm}^2$, however, the AuNP dimers reach temperatures well beyond 200°C , at which point the reduction in the thickness of the

DNA origami template is expected.³⁶ This is consistent with our observation of significant gap closure at the higher excitation intensity only.

Mapping the gap-dependent SERS signal at the single molecule level

Nanoscale control of the dimer gap size and the Raman-analyte position is critical for quantitative single-molecule SERS. To further understand the relationship between interparticle distance and SERS intensity we plotted the correlation between those two (see Figure 3). We used the strong SERS signals of the distinctive Raman peak located at 1180 cm^{-1} as the standard peak. This Raman peak is thought to arise from the polyene C-C-H deformation vibrational mode.⁴⁴ Figure 3 displays the experimental data set of SERS signals (red squares) corresponding to either the dimer structures with one dye (a and b) or four dyes (c and d) normalized to the maximum intensity. The data points were derived from measurements of individual DNA origami dimers whose gap sizes were gradually tuned using the previously described plasmonic heating protocol.

For small vibrational frequencies the Raman-scattering enhancement scales roughly with the fourth power of the electric field enhancement. Specifically, it is possible to calculate the enhancement factor (EF) as²⁴

$$EF = |E(\omega_{exc})|^2 |E(\omega_R)|^2 \quad (1)$$

where $E(\omega_{exc})$ and $E(\omega_R)$ corresponds to electrical field at the excitation and the particular vibrational shifted frequencies of the Raman signal. We used the generalized Mie theory to analytically calculate the electromagnetic field enhancement factors generated by the AuNP dimer structure as a function of the gap size. The enhancement factors are extremely sensitive to the specific position of the molecule in the structure. The DNA origami template was designed to either hold one single molecule or four molecules around the geometrical center of the dimer structure. Therefore, to obtain the theoretical SERS enhancements we calculated

the enhancements field directly at the dimer center. The black lines in Figure 3 correspond to the normalized results of this theoretical calculation.

The comparison between the experimental SERS data and the classical electromagnetic theory indicates that the observed enhancement is dominated by the pure electromagnetic effect and there is no contribution of chemical enhancement, as expected from our design where the dyes are not in direct contact with the AuNP surface. We observed approximately two orders of magnitude enhancement in the Raman scattering signal of the single molecules placed in the dimer hot spot when reducing the dimer gap size from ~ 2.5 nm to 1.4 nm. The results of multiple DNA origami AuNP dimer structures with different type and amount of dyes located in the hot spot and the different vibrational modes presented in Figure 3 and Supporting Figure 6 validate our findings. For the one-dye Cy3.5 dimer structure we monitored the fingerprints peaks of ~ 960 cm^{-1} , 1180 cm^{-1} and 1350 cm^{-1} highlighted by orange lines in Figure 2. Independently of the chosen vibrational mode (see Figure 3a, 3b and Supporting Figure 6) or the Raman reporter molecule (see Figure 3c and d) the correlation between Raman scattering intensity signals and dimer gap size are in good agreement.

We finally used fluorescence microscopy techniques to prove that our DNA origami AuNP dimers have indeed exactly one or four dyes incorporated in their structures. We measured temporal sequences of fluorescence images for the one- and four-dye-modified DNA origami structures using total internal reflection (TIR) illumination. We imaged the DNA origami structures prior to gold nanoparticle assembly to avoid quenching of the fluorescence signal of the dyes due to energy transfer processes from the molecule to the metallic particle.⁵² Figure 4 displays two representative fluorescence time traces of single DNA origami structures modified with either one (green line) or four (red line) Cy3.5

molecules. The one and four photobleaching steps of the emission traces confirm the number of dyes located in the nanoparticle hot spot.

Conclusions

We have devised a reliable approach to produce high sensitive SERS active materials that enable quantitative single molecule detection. Plasmonic heating offers the potential of producing highly reproducible nanodimers with tailored plasmonic properties. The optothermal or purely thermal effect is of general nature and can be transferred to other DNA origami based plasmonic assemblies where small gap sizes are desirable. Our approach combined with the nanometer-precise localization of individual molecules offered by the DNA origami technology is key to outline the gap size dependence of the enhanced electrical field inside the hot spot. We endorse our results by mapping the effect of the enhanced near-field on nano-sized hybrids with different numbers of dyes and different Raman reporter molecules.

Methods

Dye labeling of oligonucleotides. For the functionalization of single-stranded DNA oligonucleotides with either Cy3-Azide or Cy3.5-Azide dyes (Baseclick, Germany) the DNA staples were 5'alkyne modified (Baseclick, Germany). Here we dye labeled directly four different DNA staple sequences, which are part of the DNA origami structure. The subsequent click chemistry labeling of the alkyne-modified oligonucleotides was done *via* the Baseclick Oligo-Click –M (Baseclick, Germany) set. A detailed description can be found in the Oligo-Click-M user manual. After functionalization of the DNA staple strand with the corresponding dye, 3 washing / DNA precipitation steps with 3 M NaOAc and EtOH were

performed to remove excess unbound dyes. The concentration of the modified DNA oligonucleotide was determined *via* UV-Vis absorption spectroscopy (Nanodrop).

DNA origami folding. To fold the DNA origami template structure 10 nM of p7249 scaffold was mixed with 200 nM of each unmodified staple oligonucleotide, 10 mM Tris, 1 mM EDTA (pH 8) and 16 mM MgCl₂. The dye modified staple strands were added to the folding solution in a concentration of 400 nM to ensure incorporation into the origami structure during the folding process. Next, the folding solution was heated up to 65°C for 20 min to denature all DNA strands and then slowly cooled down to 20°C over a period of 1.5 days (1°C per 45 min). For each structure investigated here a different batch of folding solution was prepared. *E.g.* for the structure with only one dye modified staple strand incorporated in the design the other three possible strands were used in their unmodified version. After folding the DNA origami template structures they were purified from excess unbound staple strands *via* gel electrophoresis (1.0% agarose gel in 1x TAE buffer (40 mM Tris, 40 mM Acetic Acid, 1 mM EDTA, pH 8) with 11 mM MgCl₂). The bands containing the well-folded structures were cut out of the gel and the structures recovered by squeezing the cut-out gel piece.

Concentration and conjugation with DNA of AuNP. The as-bought 40 nm AuNP (BBI Solutions, 20 ml) were first concentrated and then functionalized with thiol modified DNA according to the protocol of Schreiber *et al.*⁷ In short, to the AuNP BSPP (Bis(*p*-sulfonatophenyl)phenylphosphine dihydrate dipotassium salt, Sigma-Aldrich) was added (8 mg) and stirred for three days. Then the AuNP were concentrated by adding sodium chloride (5 M) until the color of the solution turned bluish. Afterwards the solution was centrifuged (1,600 rcf, 30 min). The supernatant was removed and a washing step with 2.5 mM BSPP and methanol was performed. After a second centrifugation step the supernatant was discarded again and the concentration of the AuNP was determined *via* UV-

Vis spectroscopy (Nanodrop). In the next step the AuNP were functionalized with thiolated single-stranded DNA (ssDNA) (thiol-T19, Biomers, Germany). This step has two functions. First, the DNA functionalized AuNP are stabilized against high MgCl_2 concentrations, which are used within the DNA origami folding process and second, the sequence is used for the hybridization to the DNA origami template, which allows a site specific binding of the AuNP to the template structure. A ratio of ssDNA:AuNP of 4800:1 was used in 1x TAE buffer. The mixture was stirred 3 days on a shaker for incubation. The unbound excess of ssDNA was then removed by centrifugation of the solution with 100 kDa MWCO centrifugal filters (Amicon Ultra, Millipore, 5 min, 9,500 rcf, 400 μl 1x TAE buffer). This procedure was repeated 8 times to make sure no unbound ssDNA strands are left. To reach a high yield of attached AuNP to the DNA origami this purification step for the AuNP from unbound ssDNA was done directly before adding the AuNP to the DNA template structure. In that way the attachment points (handles) on the template structure are not blocked by unbound ssDNA.

Functionalization of DNA origami template structure with AuNP. To functionalize the template DNA origami structure at the designed attachment sites with AuNP a ratio of (DNA-modified AuNP:attachment site) of 4:1 was used. The solution was left for incubation on a shaker over 12 h at 22 C. As a last step the solution was gel purified from excess AuNP and eventually occurring agglomerates (0.7 % agarose gel in 1x TAE buffer with 11 mM MgCl_2) to obtain the final self-assembled dimer AuNP DNA origami structure. The structures were extracted from the gel by cutting out the corresponding gel band and squeezing it while recovering the liquid.

Transmission electron microscopy (TEM). To control the assembly yield the gel-purified structures were immobilized on a carbon-formvar coated TEM grid (Ted Pella) and stained with 1 % uranyl acetate for 15 seconds. To monitor a change in the dimer gap size non

stained samples were prepared. Therefore the grids were flushed with 1x TAE MgCl₂ instead of uranyl acetate. The TEM measurements were performed with a JEOL JEM-1100 electron microscope at 80 kV. For the gap size monitoring experiments (see Supporting Figure 4c) first TEM images of individual structures were taken, then the grids were heated in an oven to 200°C and afterwards the same structures were imaged again with the TEM.

Raman and Rayleigh scattering microscopy and spectroscopy. To perform the dark-field scattering spectroscopy and SERS measurements the structures were diluted to ~ 5 pM in 1x TAE, 11 mM MgCl₂ buffer and immobilized on a glass slide, which was then water flushed and nitrogen dried. Single-point Raman and Rayleigh scattering spectra were acquired in an upright Zeiss Axio Scope A1 (Zeiss) microscope equipped with an oil immersion condenser (Zeiss AxioTech 100, NA 1.2 – 1.4) and using an Acton SP2500 spectrometer (Princeton Instruments). For illumination a 100 W halogen lamp (Zeiss) was used. The microscope was adapted for Raman experiments by coupling a 612 nm CW randomly polarized laser beam (Carl Zeiss Jena, LGK7411) and using a clean-up 610 ± 10 nm bandpass filter (Laser Components) and 630 nm long pass edge filter (Laser Components, LC-630LP-25) that transmits the Raman-Stokes signal and blocks the resonant scattered laser light. An Epiplan-Neofluar 100x air objective (NA=0.9, Zeiss) was used to collect the Raman and Rayleigh scattered light, and to focus the excitation laser. The acquisition time for the Raman scattering spectra measurements was 100 s per measurement and the laser power after the objective was measured to be 150 μW, yielding a power density at the focal position of ~ 14 kW/cm². Plasmonic heating of the DNA origami gold nanoparticles dimers was possible by increasing the power density at the focal position to 60 kW/cm² and irradiating the structure for 10 sec. A cross scratch was marked on the top surface of the coverslip to assist subsequent location of the AuNP DNA origami dimers in the SEM. Dark field imaging was

recorded using a digital SLR Canon EOS 550D camera (Canon) with a resolution of 5184 x 3456 using the same objective.

Scanning electron microscopy (SEM). Gold nanoparticles DNA origami dimers immobilized on the surface of a glass coverslip were imaged in an ULTRA Series Zeiss microscope (Zeiss). Prior SEM imaging, a 2 nm gold-palladium layer was sputtered on the sample (20 seconds, 30 mA, 5 cm working distance). Imaging was performed in SE2 and InLens modes at an electron acceleration voltage of 2 kV with a working distance of ~ 3 mm.

Heating (see Supporting Figure 4d). Rayleigh scattering spectra or TEM images of gold nanoparticles DNA origami dimers deposited on the surface of a glass coverslip or a TEM grid, respectively, were acquired before and after heating. A programmable hotplate (MR Hei-Tec, Heidolph Instruments) was used to heat the samples at 200°C for 5 minutes.

Fluorescence microscopy. Total internal reflection fluorescence (TIRF) imaging experiments were conducted in borosilicate chambers with 0.6 cm² well area (sticky-Slide VI, Ibbidi) with an Olympus IX81 (Olympus) microscope. A solution of ~ 40 pM DNA origami structures (functionalized with one, two, three or four Cy3.5 dyes) was loaded into the microscope chambers immediately after flushing it with 1× TAE buffer (containing 11 mM MgCl₂). Cy3.5 fluorophores were excited with a CW TEM₀₀ 561 nm laser (Cobolt JiveTM, Cobolt AB) coupled and collimated into the microscope. A beam splitter CMR-U-M3TIR-405-488-561 (AHF) was used to reflect the excitation light into the oil immersion TIRF objective (100X, NA1.45, Olympus, Plan APO). The fluorescent signal was passed through a 600 nm long pass filter (Thorlabs) and collected with an iXon Ultra 897 EM-CCD (Andor) with 512 x 512 pixels of 16 μm x 16 μm size, operated at 100 ms per frame. Fluorescence intensity temporal time traces of single DNA origami structures were obtained with a homemade MATLAB routine⁵³.

Numerical Simulations. Optical properties of gold nanoparticle dimers were calculated with numerical solvers of the generalized Mie-Theory, implemented in Fortran⁵⁰⁻⁵¹. Two spheres with a diameter of 40 nm were placed with variable distance in a surrounding medium. The refractive index of the two particles were interpolated values of the dataset obtained by Johnson & Christy⁵⁴. For the surrounding medium an effective medium approach was used by matching the transverse plasmon mode, which is not dependent on the gap size, to the simulated plasmon peak. A value of $n = 1.4$ matched the experimental values best. The electric field was evaluated in the center between the two spheres. All simulations were averaged over both excitation parallel and perpendicular to the dimer axis. For calculating the heat profile of the dimers, the absorbed laser power was calculated with homemade Mathematica scripts from the absorption cross-section obtained from the previous simulations. The steady state-temperature of the dimers upon laser illumination was simulated with the COMSOL Multiphysics 5.2 Heat Transfer Module.

References

1. Rothmund, P. W. K., Folding DNA to Create Nanoscale Shapes and Patterns. *Nature* **2006**, *440*, 297-302.
2. Douglas, S. M.; Dietz, H.; Liedl, T.; Hogberg, B.; Graf, F.; Shih, W. M., Self-Assembly of DNA into Nanoscale Three-Dimensional Shapes. *Nature* **2009**, *459*, 414-418.
3. Hung, A. M.; Micheel, C. M.; Bozano, L. D.; Osterbur, L. W.; Wallraff, G. M.; Cha, J. N., Large-Area Spatially Ordered Arrays of Gold Nanoparticles Directed by Lithographically Confined DNA Origami. *Nat. Nanotechnol.* **2010**, *5*, 121-126.
4. Bui, H.; Onodera, C.; Kidwell, C.; Tan, Y.; Graugnard, E.; Kuang, W.; Lee, J.; Knowlton, W. B.; Yurke, B.; Hughes, W. L., Programmable Periodicity of Quantum Dot Arrays with DNA Origami Nanotubes. *Nano Lett.* **2010**, *10*, 3367-3372.
5. Maune, H. T.; Han, S.-p.; Barish, R. D.; Bockrath, M.; Goddard, I. I. A.; Rothmund, P. W. K.; Winfree, E., Self-Assembly of Carbon Nanotubes into Two-Dimensional Geometries Using DNA Origami Templates. *Nat. Nanotechnol.* **2010**, *5*, 61-66.
6. Anton, K.; Kimmo, T. L.; Päävi, T., DNA Origami as a Nanoscale Template for Protein Assembly. *Nanotechnology* **2009**, *20*, 235305.

7. Schreiber, R.; Do, J.; Roller, E.-M.; Zhang, T.; Schuller, V. J.; Nickels, P. C.; Feldmann, J.; Liedl, T., Hierarchical Assembly of Metal Nanoparticles, Quantum Dots and Organic Dyes Using DNA Origami Scaffolds. *Nat. Nanotechnol.* **2014**, *9*, 74-78.
8. Bell, N. A. W.; Engst, C. R.; Ablay, M.; Divitini, G.; Ducati, C.; Liedl, T.; Keyser, U. F., DNA Origami Nanopores. *Nano Lett.* **2012**, *12*, 512-517.
9. Wei, R.; Martin, T. G.; Rant, U.; Dietz, H., DNA Origami Gatekeepers for Solid-State Nanopores. *Angew. Chem., Int. Ed.* **2012**, *51*, 4864-4867.
10. Ke, Y.; Lindsay, S.; Chang, Y.; Liu, Y.; Yan, H., Self-Assembled Water-Soluble Nucleic Acid Probe Tiles for Label-Free Rna Hybridization Assays. *Science* **2008**, *319*, 180-183.
11. Linko, V.; Eerikainen, M.; Kostainen, M. A., A Modular DNA Origami-Based Enzyme Cascade Nanoreactor. *Chem. Commun.* **2015**, *51*, 5351-5354.
12. Surana, S.; Shenoy, A. R.; Krishnan, Y., Designing DNA Nanodevices for Compatibility with the Immune System of Higher Organisms. *Nat. Nanotechnol.* **2015**, *10*, 741-747.
13. Smith, D.; Schüller, V.; Engst, C.; Rädler, J.; Liedl, T., Nucleic Acid Nanostructures for Biomedical Applications. *Nanomedicine* **2012**, *8*, 105-121.
14. Zhao, Y.-X.; Shaw, A.; Zeng, X.; Benson, E.; Nyström, A. M.; Högberg, B., DNA Origami Delivery System for Cancer Therapy with Tunable Release Properties. *ACS Nano* **2012**, *6*, 8684-8691.
15. Schüller, V. J.; Heidegger, S.; Sandholzer, N.; Nickels, P. C.; Suhartha, N. A.; Endres, S.; Bourquin, C.; Liedl, T., Cellular Immunostimulation by Cpg-Sequence-Coated DNA Origami Structures. *ACS Nano* **2011**, *5*, 9696-9702.
16. Jungmann, R.; Avendano, M. S.; Woehrstein, J. B.; Dai, M.; Shih, W. M.; Yin, P., Multiplexed 3d Cellular Super-Resolution Imaging with DNA-Paint and Exchange-Paint. *Nat. Meth.* **2014**, *11*, 313-318.
17. Steinhauer, C.; Jungmann, R.; Sobey, T. L.; Simmel, F. C.; Tinnefeld, P., DNA Origami as a Nanoscopic Ruler for Super-Resolution Microscopy. *Angew. Chem., Int. Ed.* **2009**, *48*, 8870-8873.
18. Roller, E.-M.; Khorashad, L. K.; Fedoruk, M.; Schreiber, R.; Govorov, A. O.; Liedl, T., DNA-Assembled Nanoparticle Rings Exhibit Electric and Magnetic Resonances at Visible Frequencies. *Nano Lett.* **2015**, *15*, 1368-1373.
19. Kuzyk, A.; Schreiber, R.; Fan, Z.; Pardatscher, G.; Roller, E.-M.; Hoge, A.; Simmel, F. C.; Govorov, A. O.; Liedl, T., DNA-Based Self-Assembly of Chiral Plasmonic Nanostructures with Tailored Optical Response. *Nature* **2012**, *483*, 311-314.
20. Kuzyk, A.; Schreiber, R.; Zhang, H.; Govorov, A. O.; Liedl, T.; Liu, N., Reconfigurable 3d Plasmonic Metamolecules. *Nat. Mater.* **2014**, *13*, 862-866.
21. Acuna, G. P.; Möller, F. M.; Holzmeister, P.; Beater, S.; Lalkens, B.; Tinnefeld, P., Fluorescence Enhancement at Docking Sites of DNA-Directed Self-Assembled Nanoantennas. *Science* **2012**, *338*, 506-510.
22. Giannini, V.; Fernández-Domínguez, A. I.; Heck, S. C.; Maier, S. A., Plasmonic Nanoantennas: Fundamentals and Their Use in Controlling the Radiative Properties of Nanoemitters. *Chem. Rev.* **2011**, *111*, 3888-3912.
23. Jiang; Bosnick, K.; Maillard, M.; Brus, L., Single Molecule Raman Spectroscopy at the Junctions of Large Ag Nanocrystals. *J. Phys. Chem. B* **2003**, *107*, 9964-9972.
24. Novotny, L.; Hecht, B., *Principles of Nano-Optics*. Cambridge University Press: 2012.
25. Prinz, J.; Schreiber, B.; Olejko, L.; Oertel, J.; Rackwitz, J.; Keller, A.; Bald, I., DNA Origami Substrates for Highly Sensitive Surface-Enhanced Raman Scattering. *J. Phys. Chem. Lett.* **2013**, *4*, 4140-4145.
26. Kühler, P.; Roller, E.-M.; Schreiber, R.; Liedl, T.; Lohmüller, T.; Feldmann, J., Plasmonic DNA-Origami Nanoantennas for Surface-Enhanced Raman Spectroscopy. *Nano Lett.* **2014**, *14*, 2914-2919.
27. Pilo-Pais, M.; Watson, A.; Demers, S.; LaBean, T. H.; Finkelstein, G., Surface-Enhanced Raman Scattering Plasmonic Enhancement Using DNA Origami-Based Complex Metallic Nanostructures. *Nano Lett.* **2014**, *14*, 2099-2104.

28. Thacker, V. V.; Herrmann, L. O.; Sigle, D. O.; Zhang, T.; Liedl, T.; Baumberg, J. J.; Keyser, U. F., DNA Origami Based Assembly of Gold Nanoparticle Dimers for Surface-Enhanced Raman Scattering. *Nat. Commun.* **2014**, *5*.
29. Maier, S. A., *Plasmonics: Fundamentals and Applications*. Springer Science & Business Media: 2007.
30. Wang, Y.; Irudayaraj, J., Surface-Enhanced Raman Spectroscopy at Single-Molecule Scale and Its Implications in Biology. *Philos. Trans. R. Soc., B* **2013**, *368*.
31. Lim, D.-K.; Jeon, K.-S.; Kim, H. M.; Nam, J.-M.; Suh, Y. D., Nanogap-Engineerable Raman-Active Nanodumbbells for Single-Molecule Detection. *Nat. Mater.* **2010**, *9*, 60-67.
32. Lee, H.; Lee, J.-H.; Jin, S. M.; Suh, Y. D.; Nam, J.-M., Single-Molecule and Single-Particle-Based Correlation Studies between Localized Surface Plasmons of Dimeric Nanostructures with ~1 Nm Gap and Surface-Enhanced Raman Scattering. *Nano Lett.* **2013**, *13*, 6113-6121.
33. Lee, J.-H.; You, M.-H.; Kim, G.-H.; Nam, J.-M., Plasmonic Nanosnowmen with a Conductive Junction as Highly Tunable Nanoantenna Structures and Sensitive, Quantitative and Multiplexable Surface-Enhanced Raman Scattering Probes. *Nano Lett.* **2014**, *14*, 6217-6225.
34. Prinz, J.; Heck, C.; Ellerik, L.; Merk, V.; Bald, I., DNA Origami Based Au-Ag-Core-Shell Nanoparticle Dimers with Single-Molecule Sensitivity. *Nanoscale* **2016**, *8*, 5612-5620.
35. Urban, A. S.; Fedoruk, M.; Nedev, S.; Lutich, A.; Lohmueller, T.; Feldmann, J., Shrink-to-Fit Plasmonic Nanostructures. *Adv. Opt. Mater.* **2013**, *1*, 123-127.
36. Pillers, M. A.; Lieberman, M., Thermal Stability of DNA Origami on Mica. *J. Vac. Sci. Technol., B* **2014**, *32*, 040602.
37. Kim, H.; Surwade, S. P.; Powell, A.; O'Donnell, C.; Liu, H., Stability of DNA Origami Nanostructure under Diverse Chemical Environments. *Chem. Mater.* **2014**, *26*, 5265-5273.
38. Baffou, G.; Quidant, R., Thermo-Plasmonics: Using Metallic Nanostructures as Nano-Sources of Heat. *Laser Photonics Rev.* **2013**, *7*, 171-187.
39. Govorov, A. O.; Richardson, H. H., Generating Heat with Metal Nanoparticles. *Nano Today* **2007**, *2*, 30-38.
40. Etchegoin, P. G.; Le Ru, E. C., Resolving Single Molecules in Surface-Enhanced Raman Scattering within the Inhomogeneous Broadening of Raman Peaks. *Anal. Chem.* **2010**, *82*, 2888-2892.
41. Yu, N.-T.; Nie, S.; Lipscomb, L. A., Surface-Enhanced Hyper-Raman Spectroscopy with a Picosecond Laser. New Vibrational Information for Non-Centrosymmetric Carbocyanine Molecules Adsorbed on Colloidal Silver. *J. Raman Spectrosc.* **1990**, *21*, 797-802.
42. Yang, J. P.; Callender, R. H., The Resonance Raman Spectra of Some Cyanine Dyes. *J. Raman Spectrosc.* **1985**, *16*, 319-321.
43. Sato, H.; Kawasaki, M.; Kasatani, K.; Katsumata, M.-a., Raman Spectra of Some Indo-, Thia- and Seleno-Carbocyanine Dyes. *J. Raman Spectrosc.* **1988**, *19*, 129-132.
44. Lednev, I. K.; Fomina, M. V.; Gromov, S. P.; Stanislavsky, O. B.; Alifimov, M. V.; Moore, J. N.; Hester, R. E., A Raman Spectroscopic Study of Indolinium Steryl Dyes. *Spectrochim. Acta, Part A* **1992**, *48*, 931-937.
45. Movileanu, L.; Benevides, J. M.; Thomas, G. J., Temperature Dependence of the Raman Spectrum of DNA. Ii. Raman Signatures of Premelting and Melting Transitions of Poly(Da)·Poly(Dt) and Comparison with Poly(Da-Dt)·Poly(Da-Dt)*. *Biopolymers* **2002**, *63*, 181-194.
46. Barhoumi, A.; Zhang, D.; Tam, F.; Halas, N. J., Surface-Enhanced Raman Spectroscopy of DNA. *J. Am. Chem. Soc.* **2008**, *130*, 5523-5529.
47. Treffer, R.; Lin, X.; Bailo, E.; Deckert-Gaudig, T.; Deckert, V., Distinction of Nucleobases – a Tip-Enhanced Raman Approach. *Beilstein J. Nanotechnol.* **2011**, *2*, 628-637.
48. Chandra, A. K.; Nguyen, M. T.; Zeegers-Huyskens, T., Theoretical Study of the Interaction between Thymine and Water. Protonation and Deprotonation Enthalpies and Comparison with Uracil. *J. Phys. Chem. A* **1998**, *102*, 6010-6016.
49. Xu, L.-J.; Lei, Z.-C.; Li, J.; Zong, C.; Yang, C. J.; Ren, B., Label-Free Surface-Enhanced Raman Spectroscopy Detection of DNA with Single-Base Sensitivity. *J. Am. Chem. Soc.* **2015**, *137*, 5149-5154.

50. Ringler, M.; Schwemer, A.; Wunderlich, M.; Nichtl, A.; Kürzinger, K.; Klar, T. A.; Feldmann, J., Shaping Emission Spectra of Fluorescent Molecules with Single Plasmonic Nanoresonators. *Phys. Rev. Lett.* **2008**, *100*, 203002.
51. Xu, Y.-l.; Wang, R. T., Electromagnetic Scattering by an Aggregate of Spheres: Theoretical and Experimental Study of the Amplitude Scattering Matrix. *Phys. Rev. E* **1998**, *58*, 3931-3948.
52. Anger, P.; Bharadwaj, P.; Novotny, L., Enhancement and Quenching of Single-Molecule Fluorescence. *Phys. Rev. Lett.* **2006**, *96*, 113002.
53. Simoncelli, S.; Roberti, M. J.; Araoz, B.; Bossi, M. L.; Aramendía, P. F., Mapping the Fluorescence Performance of a Photochromic-Fluorescent System Coupled with Gold Nanoparticles at the Single-Molecule-Single-Particle Level. *J. Am. Chem. Soc.* **2014**, *136*, 6878-6880.
54. Johnson, P. B.; Christy, R. W., Optical Constants of the Noble Metals. *Phys. Rev. B* **1972**, *6*, 4370-4379.

Acknowledgements

This work has been supported by the Volkswagen Foundation, the ERC through the Advanced Investigator Grant “HYMEM” and the Starting Grant “ORCA” and the DFG through the SFB 1032 project A6 and A8. We acknowledge Paul Kühler and Arzhang Ardavan for helpful discussions.

Author Contributions

T.L. and T.L. conceived the idea and contributed to the design of the experiments. T.L., T.L. S.S and E.M.R. co-wrote the manuscript. A.J.T. and R.S. designed the DNA origami structure. E.M.R. designed and synthesized all the AuNP DNA origami dimer structures and conducted the TEM and SEM characterization. S.S. and P.U. performed the microscopy and spectroscopy experiments and analyzed the data. P.U. performed the numerical simulations. All authors contributed to the general discussion and reviewed the manuscript.

Competing Financial Interests: The authors declare no competing financial interest.

Additional Information: Supporting Information accompanies this paper. This material is available free of charges *via* the Internet at <http://pubs.acs.org>.

Figures

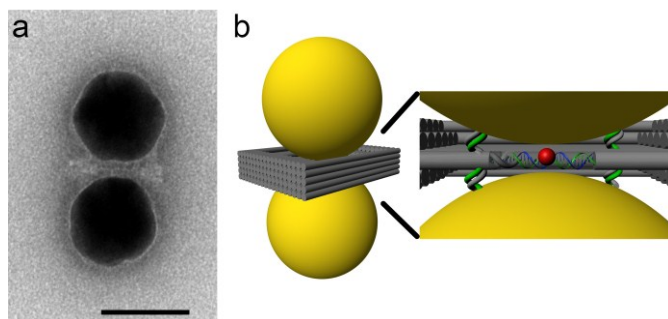


Figure 1. DNA origami AuNP dimers. (a) Representative TEM image of the plasmonic dimer nanoantenna. Scale bar 40 nm. (b) Schematic diagram of two 40 nm gold nanoparticles hosted on a 3D DNA origami structure of 47 nm x 44 nm lateral dimensions in which one or four DNA staples strands are modified with either a Cy3 or a Cy3.5 molecule.

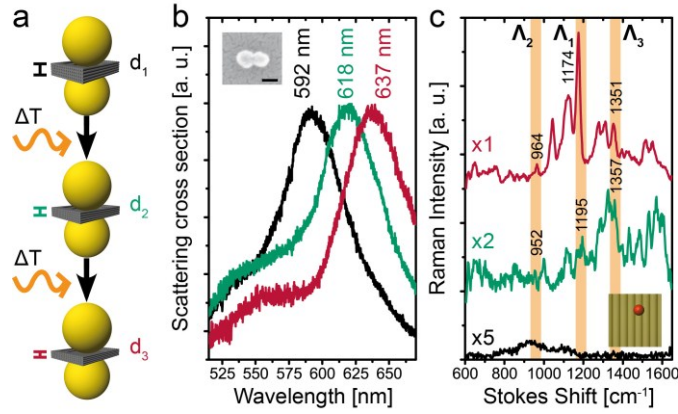


Figure 2. Laser induced gap size shrinkage. (a) Schematic representation of the experimental procedure. Representative Rayleigh (b) and Raman (c) scattering spectra of an individual dimer structure modified with a single Cy3.5 molecule placed at the hot spot before (black) and after a first (green) and a second (red) round of 10 sec laser excitation (612 nm, $\sim 60 \text{ kW/cm}^2$). The displayed values of the Raman scattering spectra have been multiplied by either 1 (x1), 2 (x2) or 5 (x5). The recorded Raman scattering signals showed the characteristic spectral fluctuations associated to single molecule SERS.⁴⁰ Inset in (b): Corresponding SEM image of the dimer structure. Scale bar 40 nm.

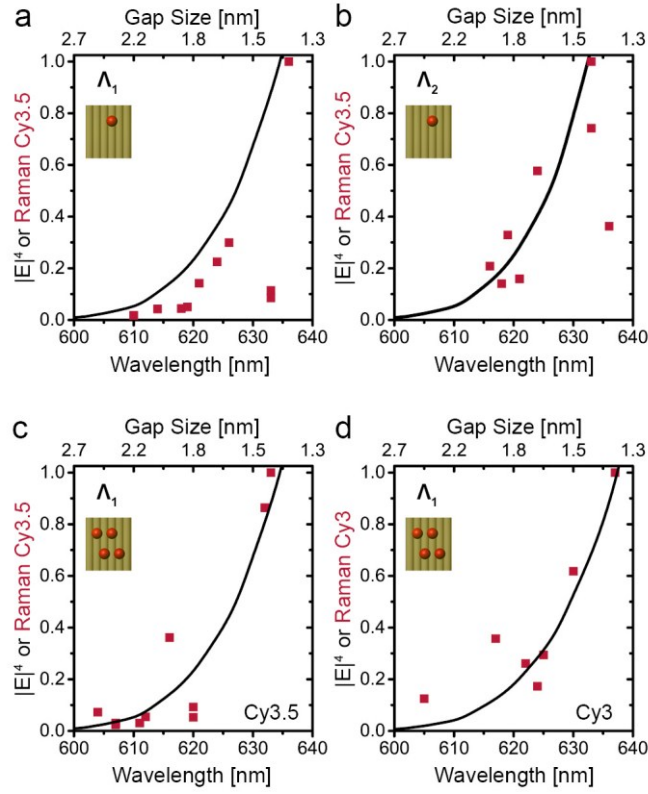


Figure 3. Mapping the gap-dependent SERS signal. Normalized Raman scattering intensities (red squares) of the vibrational modes of Cy3.5 (**a**, **b** and **c**) and Cy3 (**d**) located at Λ_1 ($\sim 1180 \text{ cm}^{-1}$) (**a**, **c** and **d**) and Λ_2 ($\sim 960 \text{ cm}^{-1}$) (**b**) as a function of the peak wavelength of the longitudinal plasmonic mode, which is related to the gap size of the DNA origami AuNP dimer. The theoretical Raman-scattering enhancement is plotted in black lines. The data points correspond to a collection of individual DNA origami dimers whose gap sizes were gradually tuned using the plasmonic heating protocol.

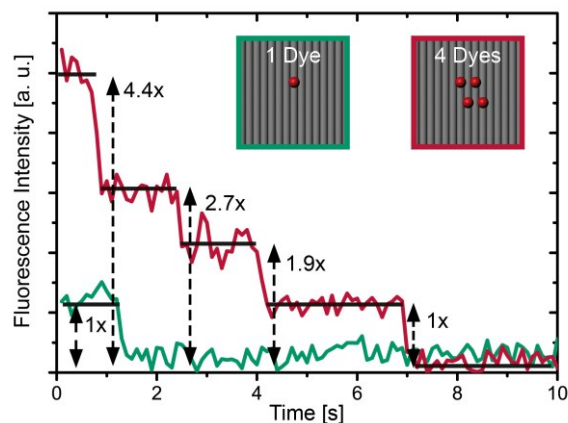


Figure 4. Single-molecule positioning validated by fluorescence microscopy.

Fluorescence intensity trajectories of single DNA origami templates modified with either one (green line) or four (red line) Cy3.5 molecules localized around the geometrical center of the structure. The inset shows a zoom in top view schematic representation of the dye-modified DNA origami designs.

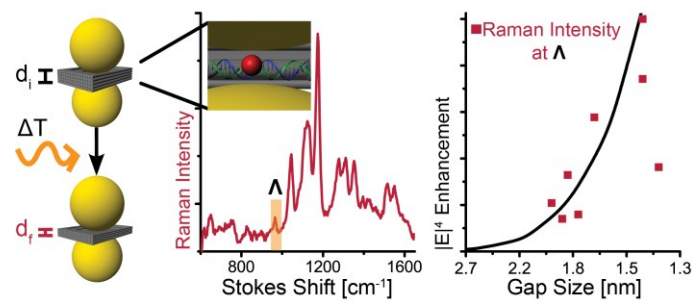


Table of Contents graphic